The Helix-Loop-Helix Protein Id1 Requires Cyclin D1 to Promote the Proliferation of Mammary Epithelial Cell Acini

C. Elizabeth Caldon,[1,2] Alexander Swarbrick,[1,2] Christine S.L. Lee,[1] Robert L. Sutherland,[1,2] and Elizabeth A. Musgrove[1,2]

[1]Cancer Research Program, Garvan Institute of Medical Research and [2]St. Vincent's Clinical School, Faculty of Medicine, University of New South Wales, Sydney, New South Wales, Australia

Abstract

Overexpression of the helix-loop-helix (HLH) protein Id1 has been associated with metastasis in breast cancer, but its role in models of early breast tumorigenesis is not well characterized. We show that the down-regulation of endogenous Id1 via proteosomal degradation and relocalization from the nucleus to the cytoplasm is an early event in the formation of mammary epithelial acini. Overexpression of Id1 in both human MCF-10A and primary mouse mammary epithelial cells disrupted normal acinar development by increasing acinar volume. This occurred in an HLH domain–dependent fashion via an increase in S phase. Id1 overexpression also increased apoptosis leading to accelerated luminal clearance, and this was reversed by coexpression of the proto-oncogene Bcl2, leading to large, disorganized structures with filled lumina. Id1 overexpression was unable to increase the volume of cyclin D1$^{-/-}$ acini, indicating that Id1 is dependent on cyclin D1 for its proliferative effects. In summary, Id1 may contribute to early breast cancer by promoting excessive proliferation through cyclin D1. [Cancer Res 2008;68(8):3026–36]

Introduction

Id proteins are helix-loop-helix (HLH) proteins that are involved in the regulation of proliferation, differentiation, apoptosis, and senescence through inhibition of HLH, Pax, and Ets transcription factors (1). HLH proteins typically dimerize to interact with DNA; however, Id proteins act as dominant negative repressors of HLH transcriptional factors and Ets/Pax proteins because they lack a DNA-binding motif.

Id proteins, in particular Id1, have been investigated as potential oncogenes because of their roles in multiple processes that are deregulated in cancer cells, including growth factor independence (2), blockade of differentiation (3, 4), and attenuation of apoptosis (5). Several potential mechanisms of cell cycle modulation by Id1 have been identified (6, 7), including effects on cyclin-dependent kinase (CDK) inhibitors (8, 9) and on cyclin D1 expression (2, 10).

High Id1 expression is strongly correlated with more aggressive or metastatic breast cancer (11–13), although some other laboratories have been unable to detect Id1 expression in breast epithelium (14). Overexpression of Id1 in breast cancer cell lines in culture increases proliferation and invasion (15, 16), and conversely, down-regulation of Id1 reduces invasiveness and metalloproteinase expression (11). Furthermore, *Id1* was included in a lung metastasis signature in a murine model of human breast cancer metastasis and was the only gene tested that increased lung metastasis when overexpressed alone (17). Conversely, Id1 antisense oligonucleotides decrease the metastatic spread of human breast cancer cells in a mouse xenograft model (11). Along with Id3, Id1 has since been shown to be required for efficient tumor initiation and lung colonization from metastatic cells derived from MMTV-Wnt1 mouse tumors (18). There is also compelling evidence that Id1 plays a crucial role in tumor angiogenesis (19), particularly in metastatic lesions (6). Overall, it seems that Id1 contributes to several facets of metastasis in breast cancer, consistent with data suggesting that Id1 contributes to metastases of gastric, epithelial ovarian, prostate, and colorectal carcinomas (20, 21).

In recent years, the generally accepted models of metastasis have undergone revision. Initially, metastatic capacity was thought to arise from mutations arising late in the disease process, after the formation of the primary invasive cancer. However, this model has been reexamined in the light of evidence that metastatic potential can be predicted from the pattern of gene expression in the primary tumor and the similarity in genetic alterations between primary and metastatic disease (22–24). Metastatic potential may thus be a feature of early cancer, albeit perhaps in a minority of cells (25, 26). An implication is that genetic alterations favoring metastasis should confer some advantage early in the oncogenic process (e.g., increased proliferative capacity that leads to a positive selection for that genetic alteration; ref. 25).

An important question relevant to the role of Id1 in metastasis is whether its overexpression has consequences that may promote the early stages of development of breast cancer. There is some evidence from studies of established cancer cell lines that Id1 overexpression may contribute to features of early oncogenesis, such as growth factor independence and increased proliferation (2). A commonly used model to address such questions is the introduction of known or suspected oncogenes into nontransformed mammary epithelial cells cultured in three dimensions, where they undergo coordinated stages of proliferation, apico-basal polarization, and luminal clearance to form acini consisting of a single layer of polarized cells surrounding a hollow lumen. Expression of proliferative or antiapoptotic oncogenes including HPV-E7 and Bcl2 leads to changes mimicking the early stages of breast carcinoma, including increased proliferation, loss of polarity, invasiveness, and luminal filling (27). We have therefore used this model system to determine whether overexpression of Id1 is capable of disrupting normal mammary epithelial cell proliferation and morphogenesis.

We have identified that Id1 is expressed in normal mammary epithelial cells and is under complex regulation during normal mammary acinar development. Importantly, the overexpression of Id1 increases proliferation within mammary epithelial acini during

Note: Supplementary data for this article are available at Cancer Research Online (http://cancerres.aacrjournals.org/).

Requests for reprints: Elizabeth A. Musgrove, Cancer Research Program, Garvan Institute of Medical Research, 384 Victoria Street, Darlinghurst, Sydney, New South Wales 2010, Australia. Phone: 61-2-9295-8328; Fax: 61-2-9295-8321; E-mail: e.musgrove@garvan.org.au.

©2008 American Association for Cancer Research.

doi:10.1158/0008-5472.CAN-07-3079

differentiation in a manner that is dependent on the presence of the Id1 HLH domain. The action of Id1 is further modulated by the presence of known oncogenes: The pro-proliferative action of Id1 is dependent on presence of cyclin D1, and overexpression of Id1 in combination with Bcl2 causes potent oncogenic transformation *in vitro*.

Materials and Methods

Retroviral vectors. The retroviral vector pMIG coexpresses the gene of interest and green fluorescent protein (GFP) from the same transcript via an internal ribosome entry site (IRES; ref. 28). pMIG was engineered to be compatible with Gateway technology (pMIG-GW; Gateway, Invitrogen) and to provide an NH_2-terminal fusion tag (pMIG-GW-V5). The *Id1, Id2*, and *cyclin D1* genes were amplified by PCR from MCF-7 cDNA and inserted into pMIG-GW or pMIG-GW-V5 using Gateway recombination (Invitrogen). Mutants of Id1 were constructed by site-directed mutagenesis with Phusion Site-Directed Mutagenesis Kit (Finnzymes) to create either nuclear localization (29) or nuclear export mutants (30), and then inserted into pMIG-GW-V5. Retroviral vectors expressing an Id1 HLH domain mutant (V98G) and NH_2-terminal and COOH-terminal truncated Id1 were constructed from vectors kindly provided by Dr. Jens Hasskarl (Department of Hematology and Oncology, University of Freiburg Medical Center, Freiburg, Germany).

Bcl2 sequences from the vector pEF-Bcl2-Puro (kindly provided by Dr. David Huang, Walter and Eliza Hall Institute of Medical Research, Melbourne, Victoria, Australia) were recombined into the pQCXIP vector (Invitrogen). The HPV-E7 gene was subcloned from pcDNA-16E7 (a kind gift of Dr. Nigel McMillan, Centre for Immunology and Cancer Research, Queensland University, Brisbane, Australia) into pMIG to give rise to pMIG-E7.

In each case, the gene sequences were verified after insertion into destination vectors by multiple DNA sequencing.

Cell culture and retroviral infection of MCF-10A cells. MCF-10A cells and MCF-10A/EcoR cells (MCF-10A cells expressing the ecotropic retroviral receptor; a kind gift of Drs. Danielle Lynch and Joan Brugge, Department of Cell Biology, Harvard Medical School, Boston, MA) were maintained in monolayer cultures as described (31, 32).

Retrovirus was generated using the ecotropic packaging cell line Phoenix-EcoR and stored at −80°C until use. Phoenix-EcoR cells transfected with pQCXIP-Bcl2 retrovirus were subjected to puromycin selection to obtain stable transfection of the retroviral constructs.

Where required, MCF-10A/EcoR cells infected with the pMIG-GW virus and its derivatives were sterile sorted by flow cytometry to obtain a 99.9% GFP-positive population. Cells infected with the pQCXIP vector and its derivatives were selected for 5 to 7 d with puromycin (2 μg/mL; Life Technologies, Inc.).

Mouse strains and genotyping. Cyclin $D1^{-/-}$ and corresponding wild-type mice (33) were the offspring of founder animals kindly provided by Dr. Clive Dickson (Cancer Research UK London Research Institute, London, United Kingdom). Animals were housed with food and water *ad libitum* with a 12-h light:12-h dark cycle at 22°C. Mammary glands were collected from mature virgin animals of at least 12 wk of age in accordance with accepted standards of humane animal care and after prior approval from the Garvan Institute/St. Vincent's Hospital Animal Ethics Committee. The genotype of experimental animals was confirmed by individual genotyping after harvesting of mammary glands and also by genotyping of pooled purified mammary epithelial cells.

Isolation, culture, and retroviral infection of primary mouse mammary epithelial cells. Mammary epithelial organoids were prepared essentially as previously described (34) and cultured overnight on collagen I–coated flasks. This resulted in an outgrowth of mouse mammary epithelial cells, which were trypsinized and replated on collagen I–coated flasks. After 8 and 24 h, the monolayer cells were infected with retrovirus. Cells were trypsinized 8 h after the secondary infection for plating onto Matrigel-coated slides. Efficacy of infection was determined by Western blotting for retrovirally expressed proteins and flow cytometric analysis of GFP expression.

Three-dimensional culture of MCF-10A cells and mouse mammary epithelial cells. For three-dimensional culture, single cells were plated onto thinly layered growth factor–reduced Matrigel (BD Biosciences) previously coated onto chamber slides (BD Falcon). MCF-10A cells were resuspended in assay medium (32) with 5 ng/mL epidermal growth factor (EGF) and overlaid on the coated slides at a density of 5,700/cm^2. Mouse mammary epithelial cells were resuspended in primary assay medium (2% FCS, 5 μg/mL insulin, 10 ng/mL EGF, hydrocortisone, cholera toxin, streptomycin, gentamicin, and 2% growth factor–reduced Matrigel) and overlaid on the coated slides at a density of 8,500/cm^2. For both cell types, this time point was taken as day 0, and the medium was replaced every 4 d.

Analysis of three-dimensional Matrigel cultures by confocal microscopy. Acini were fixed and stained as previously described (31). Primary antibodies raised against the following proteins were used to examine acinar morphology and development: activated caspase-3 (R&D Systems), cytokeratin 18 (CK18; Ks 18.04, Research Diagnostics), Ki67 (DakoCytomation), laminin V (Chemicon), and Id1 (C-19, Santa Cruz Biotechnology). Following incubation with the primary antibodies, the acini were stained with the appropriate Cy3-labeled secondary antibodies and ToPro3 as a DNA counterstain (Jackson ImmunoResearch Laboratories). Confocal microscopy was carried out on either a Leica DMRBE (SP1) or Leica DMIRE2 (SP2 AOBS) confocal microscope using either a 63× or 100× PL APO oil objective (monolayer culture), or a 40× HCX PL APO oil or immersion objective (three-dimensional culture). Images were assembled using Adobe Photoshop CS version 8.0, with minor adjustments to image contrast and intensity, where appropriate.

To quantitate acinar volume, the longest diameter of central cross-sections of each acinus was measured using Leica software, and the corresponding volume calculated. Levels of activated caspase-3 activity were quantitated by scoring on a fluorescent microscope, where acini with ≥3 activated caspase-3–positive cells were scored as positive. Alternatively, apoptosis was assessed by live cell staining of three-dimensional cultures with propidium iodide. Cultures were incubated for 30 min with 3 μmol/L propidium iodide in PBS at 37°C, 5% CO_2, before scoring acini as positive or negative on a fluorescent microscope. At least 100 acini were quantitated for each condition.

Recovery of lysates from primary culture and three-dimensional Matrigel cultures. Acini were separated from Matrigel by incubation in Matrisperse (BD Biosciences) and lysed with normal lysis buffer [50 mmol/L HEPES (pH 7.4), 1% (v/v) Triton X-100, 0.5% (w/v) sodium deoxycholate, 0.1% (w/v) SDS, 50 mmol/L sodium fluoride, 5 mmol/L EDTA, 1 mmol/L phenylmethylsulfonyl fluoride, 10 μg/mL aprotinin, 10 μg/mL leupeptin, and 1 mmol/L sodium orthovanadate], as described (32). Where appropriate, cultures were pretreated for 4 h with 52.5 μmol/L MG132 (Sigma).

Where nuclear and cytoplasmic lysates were collected, the cell pellet was resuspended in 60 μL of nuclear lysis buffer [20 mmol/L HEPES (pH 7.4), 10 mmol/L NaCl, 1.5 mmol/L $MgCl_2$, 20% glycerol, 0.1% Triton X-100, 1 mmol/L DTT, protease inhibitors] and incubated at 4°C for 5 min. The suspension was centrifuged and the supernatant (cytoplasmic fraction) removed. The remaining nuclear pellet was resuspended in 60 μL of nuclear lysis buffer and 9 μL of 5 mol/L NaCl, and incubated a further 1 h with occasional vortexing. Centrifugation at 17,530 × *g* for 10 min separated the nuclear supernatant from the insoluble pellet.

Western blot analysis. Protein lysates (10–30 μg) were separated on NuPage polyacrylamide gels (Invitrogen) and transferred onto polyvinylidene difluoride membranes. The membranes were incubated with the following primary antibodies: Id1 (C-19), c-Myc (9E10), cyclin E1 (HE12), and platelet/endothelial cell adhesion molecule 1 (M-20) from Santa Cruz Biotechnology; β-actin (AC-15, Sigma); Bcl2 (124, DakoCytomation); Bim (14A8, Calbiochem, Merck); cyclin D1 (DCS6, Novocastra); CK18 (Ks 18.04, Research Diagnostics); glyceraldehyde-3-phosphate dehydrogenase (GAPDH; 4300, Ambion); GFP (ab6658, Abcam); growth factor receptor binding protein 2 (Grb2; G16720), $p21^{Waf1/Cip1}$ (C24420), and $p27^{Kip1}$ (K25020) from BD Transduction Laboratories; and V5 (R960-25, Invitrogen).

The secondary antibodies were horseradish peroxidase–conjugated sheep α-mouse, donkey α-rabbit (Amersham Biosciences), donkey α-goat (Santa Cruz Biotechnology), and rabbit α-rat (Pierce), and specific proteins were visualized by chemiluminescence (Perkin-Elmer). Densitometry was done using IPLab Gel software (Scanalytics, Inc.). Images were assembled using Adobe Photoshop CS version 8.0.

Flow cytometry. Acini were recovered, disassociated, stained, and analyzed by flow cytometry essentially as described in ref. 32.

Statistical analysis. Statistical analysis was carried out with StatView 4.02 (Abacus Concepts, Inc.). Differences between groups were evaluated by Fisher's protected least significant difference test after ANOVA repeated measures analysis.

Results

Id1 regulation during mammary acinar development. There are conflicting reports on whether Id1 is expressed in the epithelial (2, 4, 11, 35) or endothelial (14, 19, 36) cells within the mammary gland. We were able to reliably detect Id1 mRNA and protein expression in a range of normal and immortalized human mammary epithelial cells by Western blotting, reverse transcription-PCR, or immunofluorescence (Supplementary Fig. S1*A* and *B*; Fig. 1), in concordance with the majority of studies (2, 4, 11, 12, 35). Importantly, Id1 was also detected by Western blotting in the purified epithelial fraction of mouse mammary glands, showing that the expression of Id1 in cell lines is not a cell culture artifact (Supplementary Fig. S1*C*).

The activity of Id1 is regulated by translocation in several cell types (37). Confocal imaging showed that in both MCF-10A cells and primary mouse mammary epithelial cells in three-dimensional culture, Id1 underwent a marked translocation to the cytoplasm as early as day 4 of morphogenesis (Fig. 1*A* and data not shown). Western blotting of nuclear and cytoplasmic lysates collected from two-dimensional and three-dimensional cultures also showed altered localization of Id1 (i.e., Id1 was both nuclear and cytoplasmic in two-dimensional culture, but became predominantly cytoplasmic in three-dimensional culture; Fig. 1*B, top*), and the cytoplasmic translocation became more pronounced with extended culture (Supplementary Fig. S2*A*). Immunofluorescence of mouse mammary gland sections confirmed that Id1 was also cytoplasmic in mouse mammary epithelium *in vivo* (Fig. 1*C*). Furthermore, Id1 was colocalized with the luminal epithelial marker CK18, identifying that Id1 was specifically expressed in the luminal epithelial cells of the mouse mammary gland (Fig. 1*C*).

Id1 localization may be directed by numerous factors, including active nuclear localization (NLS; ref. 29) and nuclear export (NES; ref. 30) sequences and the localization of binding partners (38). The translocation of Id1 to the cytoplasm directed Id1 away from its known HLH-binding partner and target for inhibition, E2A (38), which was localized to the nucleus both in two-dimensional and three-dimensional cultures (Fig. 1*A*), indicating that there are other factors directing Id1 localization in mammary epithelial acini. We further investigated the regulation of Id1 localization by expressing V5-tagged Id1 mutants that either lack the NLS or NES sequences, are unable to bind HLH proteins (Id1-V98G; ref. 39), or lack either the NH_2- or COOH-terminal domains (Id1-ΔNH_2 and Id1-ΔCOOH; ref. 39). Western blotting of nuclear and cytoplasmic lysates from cells expressing these mutants identified that disruption of the HLH domain and introduction of NES and NLS mutations reduced the proportion of nuclear Id1 in monolayer culture (Fig. 1*B*). Due to the close proximity of these three sets of mutations within the HLH domain, it is difficult to determine whether disruptions of the localization domains independently affect localization, or whether all three mutations may disrupt binding to certain HLH partner proteins. For this reason, we concluded that mutations within the HLH domain prevent proper localization of Id1 to the nucleus in monolayer culture. The Id1-ΔNH_2 mutant showed localization similar to endogenous protein, if with slightly reduced proportions of nuclear Id1-ΔNH_2 in monolayer culture (Fig. 1*B*). By contrast, the Id1-ΔCOOH mutant had similar localization to endogenous Id1 in monolayer culture, but had an increased proportion of nuclear protein in three-dimensional culture (Fig. 1*B*). This suggests that the COOH-terminal domain, which has not been well characterized to date, may include regions that are important for cytoplasmic localization. Id2, a related but functionally distinct Id protein (4), also showed distinct localization patterns from Id1: It was distributed throughout the nucleus and the cytoplasm in both two-dimensional and three-dimensional cultures (Fig. 1*B*). Consequently, the localization of Id1 in mammary epithelial acini is under unique regulation that is not general to all Id family members and is dependent on its HLH domain for nuclear localization in mammary epithelial cells, and loss of the COOH-terminal domain of Id1 reduces cytoplasmic translocation in three-dimensional culture.

Because Id1 is down-regulated during the differentiation of a number of cell types (40), we investigated the expression levels of Id1 in the MCF-10A model. The Id1 protein showed an early decrease in expression on transfer to three-dimensional culture followed by a steady decrease through to day 20 of the time course (Supplementary Fig. S2*B*; Fig. 2*A*). To determine whether the decreasing levels of Id1 were due to protein degradation, we treated MCF-10A acini with the proteosomal inhibitor MG132 for 4 hours. This resulted in a significant accumulation of Id1 protein in both the nucleus and cytoplasm, consistent with ubiquitin-mediated degradation (Fig. 1*D*). Absolute levels of Id1 in maturing MCF-10A acini are thus reduced through directed degradation, whereas active nuclear levels of Id1 are further reduced through sequestration in the cytoplasm.

Effect of overexpression of Id1 on mammary epithelial cells in three-dimensional culture. To investigate the effect of Id1 overexpression, we infected MCF-10A-EcoR cells with an Id1-IRES-GFP retrovirus (Id1) or the corresponding control virus (vector) and selected GFP-positive populations by fluorescence-activated cell sorting. These populations were plated onto Matrigel to examine the effect of Id1 overexpression on three-dimensional culture. Id1 was down-regulated during acinar morphogenesis even when overexpressed (Fig. 2*A*); however, the retroviral overexpression of Id1 resulted in at least 2-fold higher levels of Id1 throughout the time course (Fig. 2*B*). There was a significant increase in nuclear protein in three dimensions, although the majority of overexpressed protein was cytoplasmically localized, so that overexpressed Id1 was localized in the same way as endogenous protein (Fig. 2*C*).

Id1-overexpressing acini seemed to be morphologically similar to control, with a polarized outer layer of epithelium and normal deposition of a laminin V basement membrane. They were, however, ~50% larger in volume than vector control acini throughout the time course (Fig. 2*D*; $P < 0.0001$). When Id2 was overexpressed in parallel, it had the opposite effect of decreasing acinar volume (data not shown).

Overexpression of a HLH-incompetent Id1 in mouse mammary epithelial cells. To confirm and extend these observations, we also expressed Id1 in mouse mammary epithelial

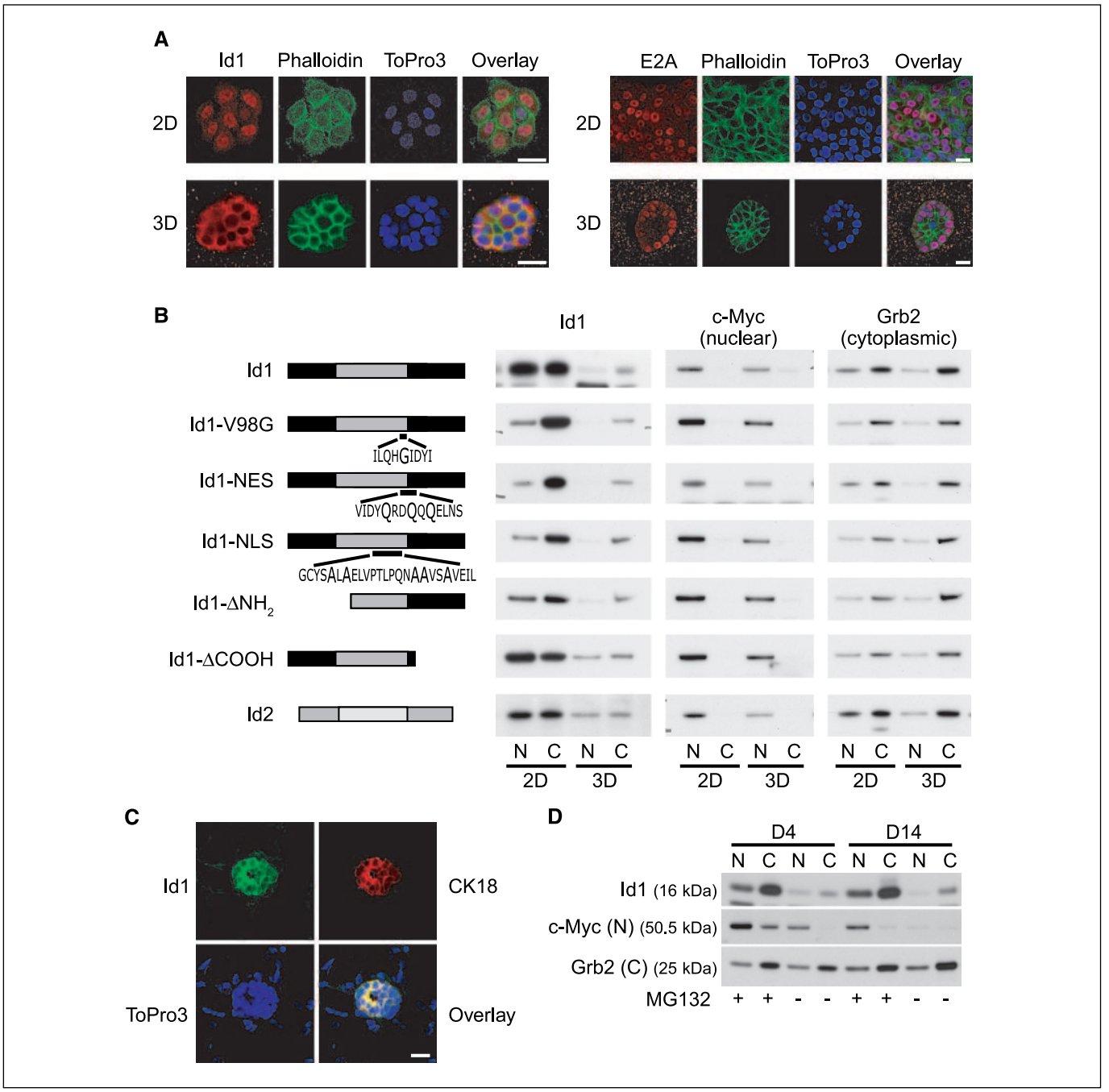

Figure 1. Id1 is dynamically regulated during MCF-10A acinar morphogenesis by both localization and turnover. Representative of up to four experiments. *A,* cells grown in either two-dimensional or three-dimensional culture were fixed after 4 d of culture. Slides were probed with either Id1 or E2A antibodies (*red*), counterstained with phalloidin (*green,* actin) and ToPro3 (*blue,* nuclei), and imaged on a confocal microscope. *Bar,* 20 μm. *B,* V5-tagged Id1 mutants were overexpressed in two-dimensional (3 d) and three-dimensional (6–7 d) cultures, including Id1-V98G, Id1-NES, Id1-NLS, Id1-ΔNH_2, and Id1-ΔCOOH, as well as Id2. Nuclear and cytoplasmic lysates were immunoprobed with α-V5. Lysates from parental MCF-10A cells cultured in parallel were probed with α-Id1. c-Myc and Grb2 were used as positive controls for nuclear and cytoplasmic fractions, respectively. *C,* immunofluorescence analysis of alveoli from mouse mammary glands of day 12 of pregnancy. Id1 (*green*) colocalizes with luminal epithelial marker CK18 (*red*). Nuclei of cells stained with ToPro3 (*blue*). *Bar,* 20 μm. *D,* MCF-10A cells were pretreated with 52.5 μmol/L MG132 for 4 h before harvest and then immunoprobed for Id1. c-Myc and Grb2 were used to indicate efficient separation of the nuclear and cytoplasmic fractions, respectively.

cells. After purification and initial short-term monolayer culture, when cultured in three dimensions, these cells underwent acinar development that occurred over a more rapid time course but otherwise mimicked the well-characterized process of acinar development in MCF-10A cells. Small balls of cells were apparent within 2 to 3 days, and luminal clearance began at day 3. By day 6, the acini appeared to be fully formed and consisted of a single layer of outer polarized cells surrounding a hollow lumen (see Fig. 3*B*). The acini were confirmed to be epithelial by CK18 immunofluorescence (data not shown).

Mouse mammary epithelial cells were then infected with retrovirus expressing GFP alone (vector control), Id1-V5, or Id1

V98G-V5, the Id1 mutant unable to bind HLH domains. Cells successfully infected with the retrovirus could be identified by coexpression of GFP and accounted for 12% to 25% of each population, as analyzed by flow cytometry. Expression was confirmed by Western blotting for Id1, V5, and GFP (Fig. 3*A*). Again, the introduction of Id1 did not alter acinar structure, but acini overexpressing Id1-V5 showed a significant increase in acinar volume compared with vector control and Id1 V98G-V5 ($P < 0.0018$; Fig. 3*B* and *C*). Id1 V98G-V5–expressing acini did not show any volume or structural changes compared with vector control acini ($P < 0.73$), indicating that the phenotypic changes caused by Id1 are dependent on an intact HLH domain. Overexpression of Id1 lacking the V5 tag also significantly increased acinar volume ($P < 0.0001$) when overexpressed in mouse mammary epithelial cells (see Fig. 6*D*). Thus, the results from primary mouse mammary epithelial cells recapitulated the effects seen in MCF-10A human immortalized mammary epithelial cells, and further identified that the Id1 HLH domain was necessary for Id1 to promote an increase in acinar volume.

Effect of Id1 overexpression on proliferation, differentiation, and apoptosis in MCF-10A cells. We next analyzed the rates of proliferation and apoptosis in acini overexpressing Id1 to further investigate the Id1-mediated increase in acinar volume. We did not observe any obvious effects of Id1 overexpression in MCF-10A cells in three-dimensional culture on cyclins D1 and E or the CDK inhibitors $p21^{Waf1/Cip1}$, $p27^{Kip1}$, and $p57^{Kip2}$ (Fig. 2*A*). However, Id1-overexpressing acini isolated from day 6 cultures and analyzed by flow cytometry had a significantly higher S phase than vector control acini ($P < 0.001$; Fig. 4*A*). This indicates that the change in acinar volume was likely due to an increase in cell proliferation rather than any change in cell size.

Id1 overexpression also increased the rate of luminal clearance of MCF-10A acini. Figure 4*B* shows representative Id1-overexpressing acini at day 4, where one acinus is already showing the formation of a luminal pocket and two acini have marked activated caspase-3 activity (*arrows*). By comparison, at this time point, the vector control acini did not show luminal clearance and had barely detectable activated caspase-3 immunoreactivity. Quantitation of

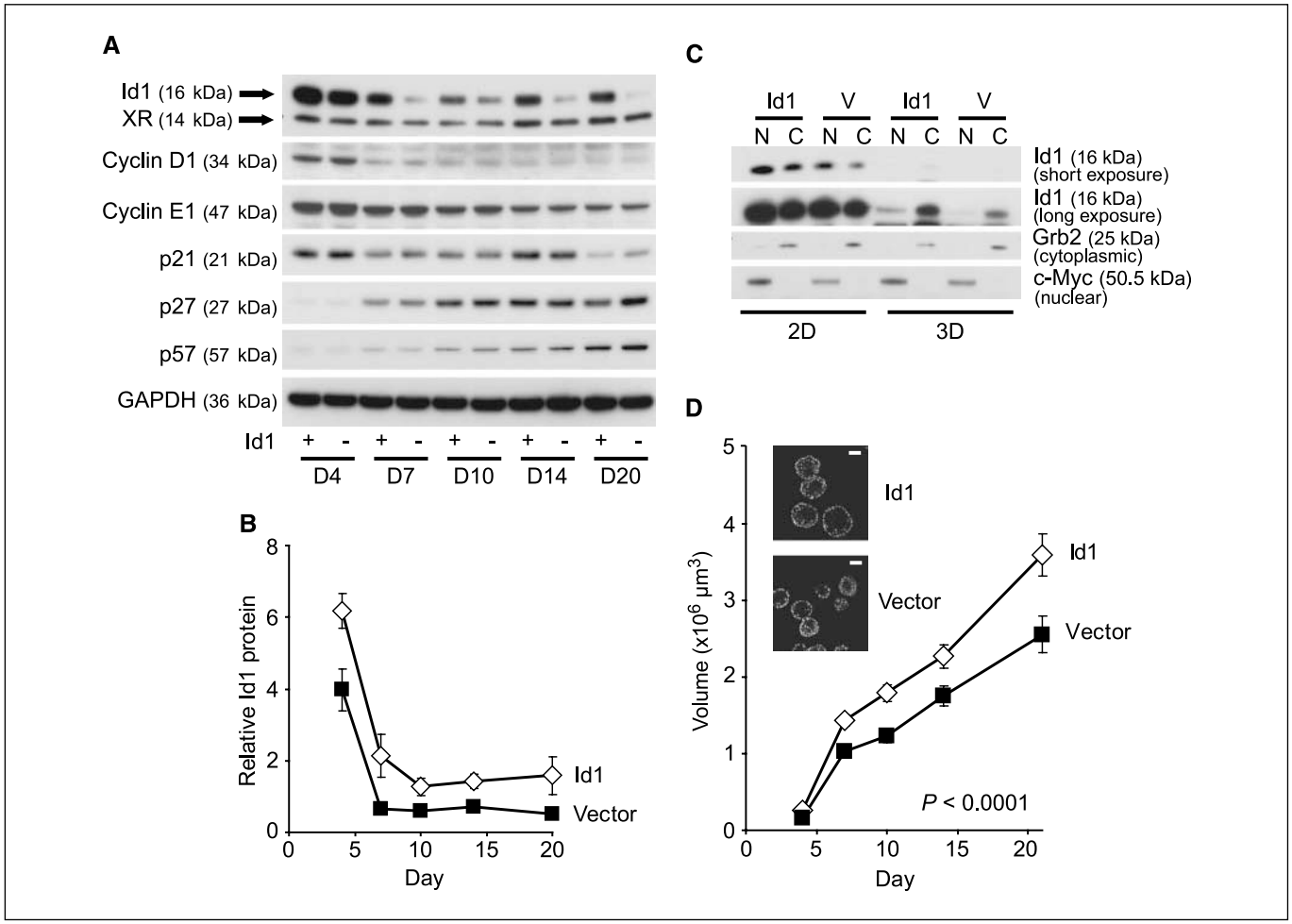

Figure 2. Overexpressed Id1 induces an increase in acinar volume. Id1 and vector control MCF-10A cells were cultured in three dimensions, and cells collected at 4, 7, 10, 14, and 20 d. *A,* lysates were probed with antibodies to Id1, cyclin D1, cyclin E1, $p21^{Waf1/Cip1}$, $p27^{Kip1}$, and $p57^{Kip2}$. GAPDH immunoblotting was done to indicate equal loading. *XR,* cross-reacting band. *B,* Id1 protein levels were quantitated by densitometry and normalized for loading using GAPDH. Data were pooled from five independent experiments. *Bars,* SE, where this is greater than the size of the symbol used. *C,* nuclear and cytoplasmic lysates collected from two-dimensional (day 3) and three-dimensional (day 7) cultures of MCF-10A cells overexpressing either Id1 or vector control were immunoprobed for Id1. c-Myc and Grb2 were used as positive controls for nuclear and cytoplasmic fractions, respectively. *D,* Id1 and vector acini were fixed and imaged for nuclear staining (ToPro3) using a confocal microscope. For each time point, the diameters through the largest confocal cross section of at least 100 structures were measured and the equivalent volume was calculated. Representative of five experiments. *Bars,* SE. *Inset,* representative cross sections of day 14 acini. *Bar,* 40 μm.

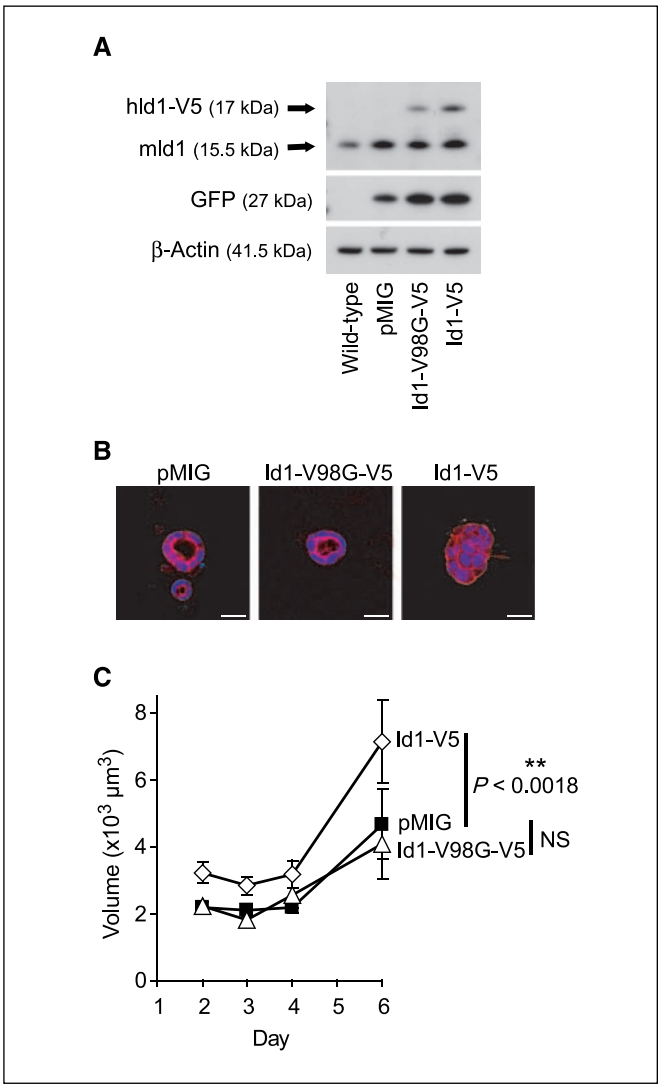

Figure 3. Id1 requires its HLH domain to promote proliferation in mammary epithelial acini. Primary mouse mammary epithelial cells were infected with Id1-V5, Id1-V98G, or vector control and plated for three-dimensional culture on Matrigel for a time course of 6 d. Representative of two experiments. *A,* protein lysates from each cell line were immunoblotted with α-Id1 and α-GFP. β-Actin immunoblotting was used to indicate equal loading. *hId1,* human Id1; *mId1,* mouse Id1. *B,* acini were fixed and stained with phalloidin (*red*) and ToPro3 (*blue*) and subsequently imaged with a confocal microscope. Representative cross-section images of day 6 acini. *Bar,* 20 μm. *C,* for each time point, the diameters through the largest confocal cross section of at least 100 structures were measured and the volume was calculated. *Bars,* SE.

the number of activated caspase-3–positive acini showed that the Id1-overexpressing population had significantly higher activity at days 4, 7, and 10 (Fig. 4*C*). Lysates collected throughout the time course were blotted for markers of apoptosis, and we identified a decrease in Bcl2 expression concurrent with Id1 overexpression (Fig. 4*D*). By contrast, there were no changes in expression of the known MCF-10A apoptotic regulator Bim (41) with Id1 overexpression, indicating that changes in apoptosis are targeted through Bcl2 (Fig. 4*D*).

Members of the Bcl family are known downstream targets of Id1 activity (5) and also cooperate with Id proteins in promoting cell immortalization (42). Because Id1 overexpression seemed to accelerate luminal clearance in a manner that may be facilitated by Bcl2, we coexpressed Id1 and Bcl2 in MCF-10A cells (Fig. 5*B*) and examined their morphology in three-dimensional culture (Fig. 5*A*). Using live cell propidium iodide staining, we identified that Bcl2-overexpressing acini exhibited a delay in luminal clearance, as previously reported (ref. 43; Fig. 5*C*). Acini coexpressing Id1 and Bcl2 exhibited both delayed luminal clearance and increased acinar volume, consistent with an additive effect of the expression of the two proteins (Fig. 5*A, C*, and *D*). Moreover, the acini overexpressing both Id1 and Bcl2 had a disorganized appearance; many acini had multiple protusions and lacked overall symmetry (Fig. 5*A*). MCF-10A cells coexpressing HPV-E7 and Bcl2 cultured in parallel also formed large structures with filled lumina (Fig. 5*A*), as previously reported (43). However, these structures were symmetrical and lacked the disorganization exhibited with coexpression of Id1 and Bcl2, indicating that this is a specific effect of Id1 rather than a consequence of deregulated proliferation.

Overexpression of Id1 on a *cyclin D1*$^{-/-}$ background. Cyclin D1 has been implicated in several cell types as a target of Id1 (2, 10) and is a key modulator of changes in proliferation. Furthermore, Ras can either increase or depend on Id1 expression in some model systems (44, 45), and cyclin D1 dependence is a feature of mammary oncogenesis induced by Ras (46, 47). Thus, whereas Id1 overexpression does not overtly increase cyclin D1 levels, Id1 may require cyclin D1 for its effects on proliferation.

Therefore, we investigated whether Id1 is dependent on cyclin D1 for its effects on proliferation in three-dimensional culture. We infected mouse mammary epithelial cells derived from *cyclin D1*$^{-/-}$ and wild-type mice with retrovirus containing either Id1-IRES-GFP or a control vector. Western blotting confirmed the expression of Id1 and cyclin D1 in the appropriate populations (Fig. 6*A*). The populations of GFP-positive acini (wild-type vector, wild-type Id1, *cyclin D1*$^{-/-}$ vector, and *cyclin D1*$^{-/-}$ Id1) were observed throughout the 6-day time course of differentiation and compared for differences in structure and volume (Fig. 6*B* and *C*). When Id1 was overexpressed in wild-type mouse mammary epithelial cells, acinar volume was increased, consistent with data in Figs. 2 and 3. When Id1 was overexpressed on the *cyclin D1*$^{-/-}$ background, however, there was no increase in acinar volume compared with the vector-infected cells ($P < 0.667$, Fig. 6*B* and *C*). Thus, the increase in proliferation that is caused by Id1 overexpression is dependent on cyclin D1.

We also noted that the *cyclin D1*$^{-/-}$ acini, although normal in appearance, were significantly smaller than wild-type acini by the end of the assay (Fig. 6*D*), consistent with the impaired proliferation observed in *cyclin D1*$^{-/-}$ mammary glands *in vivo* (33). (33). To show that *cyclin D1*$^{-/-}$ acini are not generally refractory to increases in proliferation, we overexpressed human cyclin D1 in *cyclin D1*$^{-/-}$ mouse mammary epithelial cells and cultured the cells in three-dimensions (Supplementary Fig. S3*A* and *B*). In parallel, we expressed Id1 and a vector control in mouse mammary epithelial cells and measured acinar volume after 6 days of culture on Matrigel. Overexpression of cyclin D1 led to an increase in acinar size on both a *cyclin D1*$^{-/-}$ and a wild-type background compared with vector control, indicating that *cyclin D1*$^{-/-}$ acini can be induced to further proliferate with the appropriate stimuli (Fig. 6*D*; Supplementary Fig. S3*C*). By contrast, Id1 was only able to increase acinar size in wild-type cells (Fig. 6*B–D*; Supplementary Fig. S3*C*), further confirming our observation that Id1 requires cyclin D1 to stimulate proliferation in mammary epithelial acini.

Discussion

High expression of Id1 has a well-established correlation with both angiogenesis and metastasis in breast cancer. An unresolved question is whether Id1 is expressed and functionally important in mammary epithelium, and whether its expression contributes to transformation in early breast cancer. Here, we show that Id1 acts in mammary epithelial cells to drive cyclin D1–dependent proliferation, and when overexpressed, leads to excessive proliferation.

Using the MCF-10A model system, we have identified that the down-regulation of nuclear Id1 via ubiquitin-mediated degradation and cytoplasmic relocalization is an early event in the differentiation of mammary epithelium. HLH transcription factors are generally nuclear, as we have shown here for the known Id1 binding partner E12/E47 (38), and the cytoplasmic relocalization of Id1 would disrupt its ability to interact with and inhibit nuclear binding partners during differentiation. The cytoplasmic translocation of Id1 was not dependent on its HLH domain; instead the COOH-terminal domain seemed to potentially play a role in tethering Id1 in the cytoplasm. Id proteins are known to be sequestered by cytoplasmic proteins in other cell types (48), providing a potential mechanism for the localization of Id1 to the cytoplasm in three-dimensional culture and *in vivo*.

Overexpression of Id1 led to a significant increase in the volume of either primary mouse mammary epithelial acini or MCF-10A human breast epithelial cell acini. This occurred in an HLH-dependent fashion, implying that Id1 exerts its pro-proliferative effects through a binding partner. Mist-1 (14) and ITF-2 (35) are potential mammary-specific Id1 binding partners. However, neither of these proteins promotes growth arrest when overexpressed (14, 49), and so interference with their DNA-binding ability is unlikely to account for a pro-proliferative effect of Id1 overexpression. The binding partner of Id1 necessary for its pro-proliferative effects thus remains unknown.

The increase in acinar volume induced by Id1 was associated with an increase in S phase of acinar cells. A major mechanism by

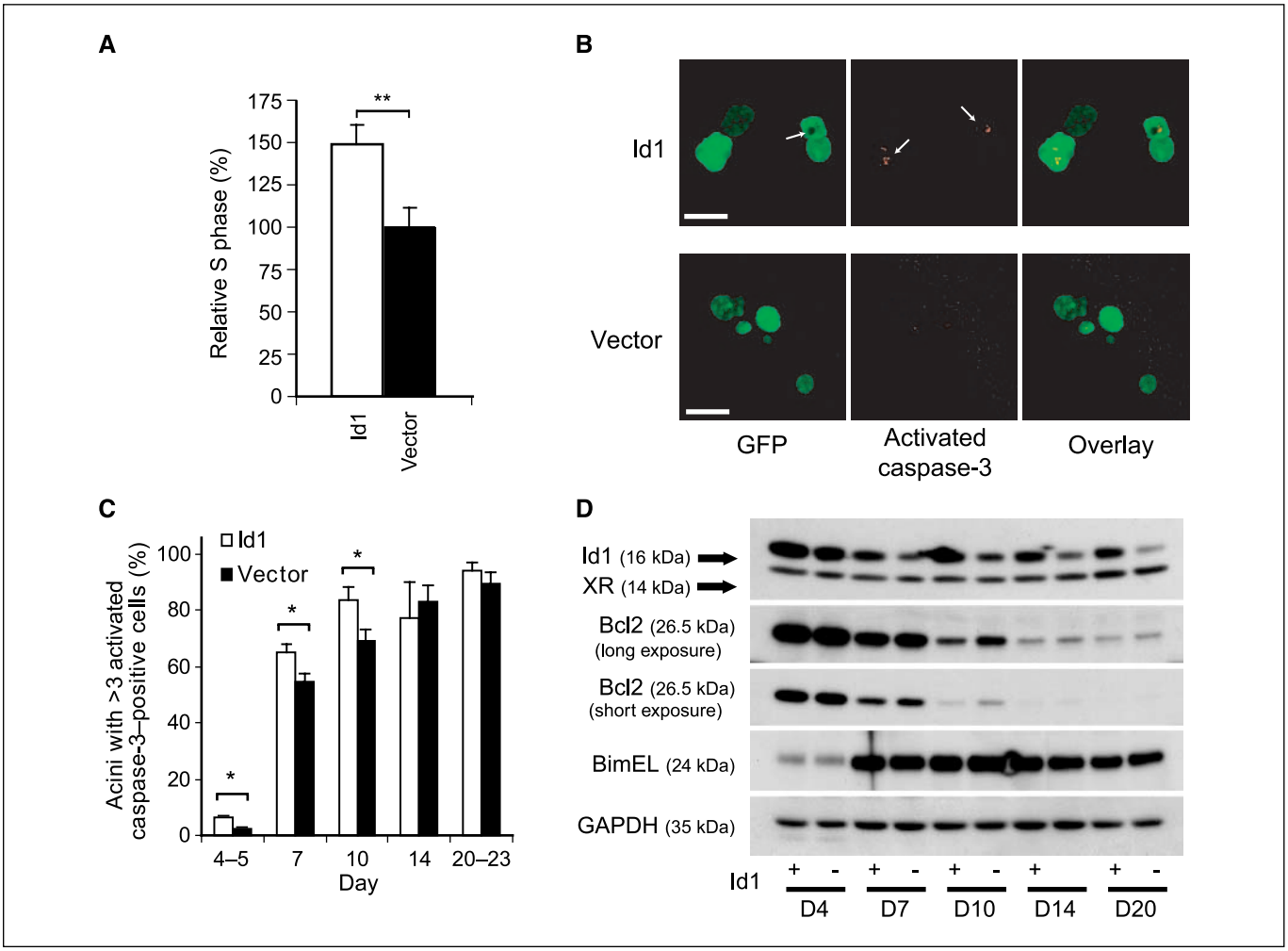

Figure 4. Id1 overexpression in MCF-10A acini alters proliferation and apoptosis. Id1 and vector control MCF-10A cells were three-dimensionally cultured on Matrigel. *A,* acini collected at day 6 were dissociated and stained with propidium iodide. S phase was determined from quantitating DNA histograms generated from flow cytometric analysis. Data were pooled from six experiments. **, $P < 0.001$. *B,* acini were fixed and immunostained with activated caspase-3 (*red*) before imaging with a confocal microscope. Representative cross sections of day 4 acini. *Green,* GFP. *Bar,* 25 μm. *C,* fixed and stained acini from 4 to 5, 7, 10, 14, and 20 to 23 d of culture were quantitated for activated caspase-3 expression using an epifluorescent microscope. Acini with ≥3 activated caspase-3–positive cells in the lumen were deemed positive. Data were pooled from five independent experiments. *Bars,* SE, *, $P < 0.05$. *D,* lysates were collected over a 20-d time course and immunoprobed for Id1, Bcl2, Bim, and GAPDH. Only the BimEL isoform is detected in MCF-10A cells; see ref. 41.

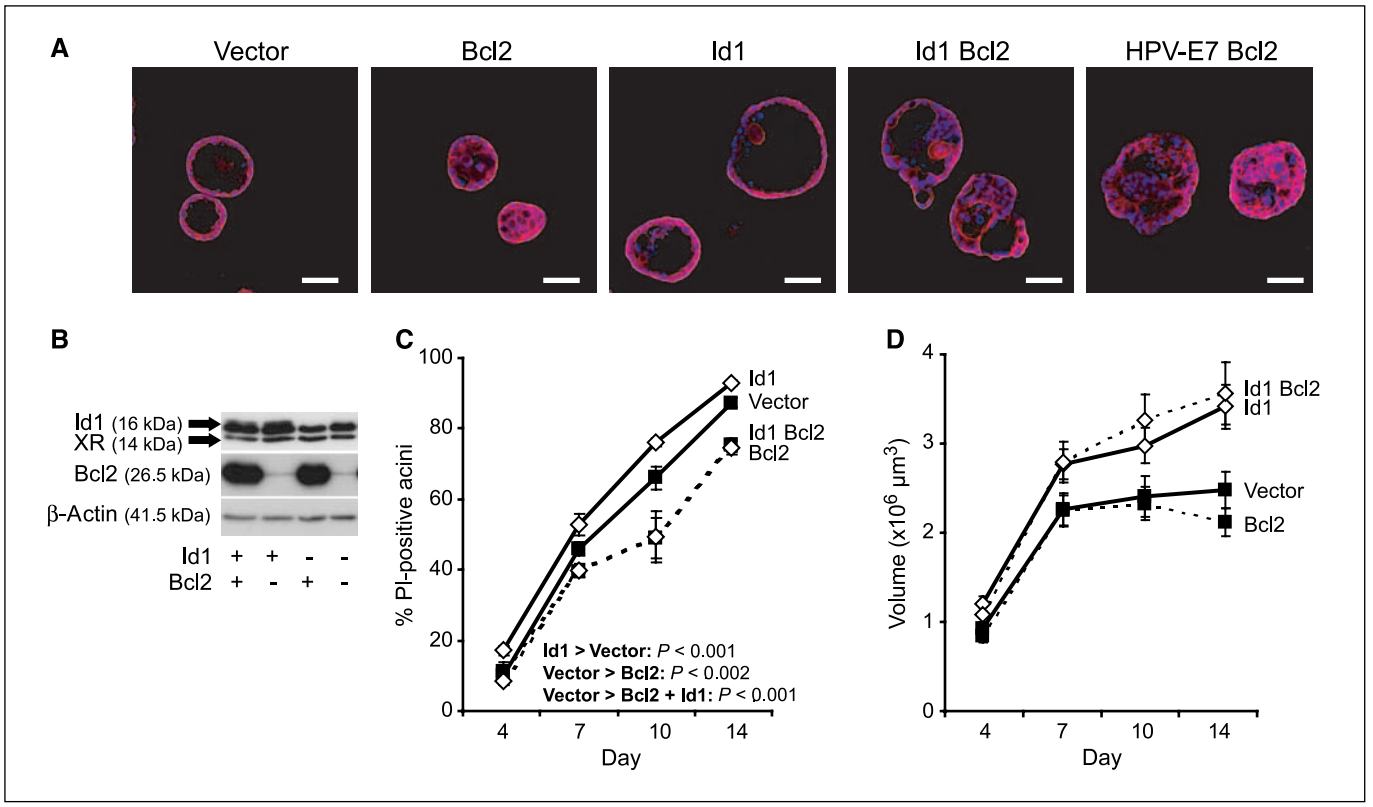

Figure 5. The coexpression of Id1 and Bcl2 in MCF-10A three-dimensional culture leads to a more transformed phenotype. MCF-10A cells expressing Id1, Bcl2, Id1 + Bcl2, or vector control were cultured on Matrigel over a time course of 20 d. Representative of three experiments. *A,* representative cross-section images of each cell type at 20 d, as well as HPV-E7 + Bcl2 infected MCF-10A cells. *Red,* activated caspase-3; *blue,* ToPro3; *green,* GFP. *Bar,* 100 μm. *B,* monolayer lysates of each cell type were Western blotted for Id1, Bcl2, and β-actin. *C,* acini from the indicated time points were stained with propidium iodide (*PI*) and positive staining was quantitated with an epifluorescent microscope. At least 80 structures were quantitated per time point. *Bars,* SE. *D,* for each time point, the diameters through the largest confocal cross section of at least 100 structures were measured and the volume was calculated. Representative experiment. *Bars,* SE.

which Id1 modulates the cell cycle is through regulation of $p16^{INK4A}$; however, this gene is deleted in MCF-10A cells (31). In different cell types, Id1 also modulates signaling pathways including transforming growth factor β (50), nuclear factor κB (10), and EGF receptor (51) that target cell cycle proteins such as cyclins and CDK inhibitors. In MCF-7 breast cancer cells, Id1 down-regulation leads to decreased expression of cyclins D1 and E1 and consequent decrease in cyclin-CDK activity (2). However, none of these identified cell cycle targets of Id1 were detectably affected in MCF-10A acini overexpressing Id1. It is possible that changes in cyclin and CDK inhibitor proteins were too subtle to be detected by Western blotting. However, given that both acinar volume and S phase are significantly increased with Id1 overexpression, it is also possible that cell proliferation is being altered by another as yet undefined mechanism.

The absence of cyclin D1 can inhibit mammary tumorigenesis driven by Neu or Ras, but not that driven by Wnt or c-Myc (47), arguing that cyclin D1 is a necessary component of certain oncogenic processes, but not of others. The absence of cyclin D1 prevented any Id1-mediated increase in acinar volume, indicating that Id1 requires cyclin D1 for its proliferative effects. Id1 may potentiate the action of cyclin D1 rather than increasing its expression because cyclin D1 levels did not seem to increase in response to Id1 overexpression in MCF-10A cells, consistent with the previous observation that D-type cyclins are not always induced during transformation by oncogenes that require their expression (46). Similarly, Id1 is required for competence of Ras-mediated effects in fibroblasts, although Id1 is not able to directly alter levels of target genes per se (45). It will be interesting to test whether Id1 is a mediator of Ras signaling in mammary epithelial cells, as it lies downstream of Ras in other tissues (45) but depends on the known Ras-target cyclin D1 in mammary epithelial acini.

In several model systems, Id1 overexpression delays differentiation while enhancing proliferation (3), including studies in mammary epithelial cells that suggest that Id1 can indeed suppress differentiation, as measured by the expression of β-casein, and induce disaggregation (3, 4, 35). Surprisingly, Id1 overexpression, while increasing the S phase of MCF-10A cells in three-dimensional culture, also seems to accelerate progression to maturity through the induction of luminal apoptosis. Other pro-proliferative oncogenes such as cyclin D1 and HPV-E7 also lead to larger structures with cleared lumens, where the increase in apoptosis is believed to be coupled to the increase in proliferation (43). Id1-induced hyperproliferation may also be indirectly compensated by an increase in luminal clearance, such that the Id1-overexpressing acini form into normal, but larger, structures. However, Id1 may also have a functional role in luminal apoptosis because we have observed that Id1 overexpression induced down-regulation of Bcl2, consistent with observations that Id1 overexpression induces apoptosis in dense cultures of mammary epithelial cells (35) and in rat embryo fibroblasts where induction of apoptosis was closely linked to cell cycle state (42). Id1 is also highly expressed during

involution of the mammary gland, again consistent with its potential functional role in apoptosis (35).

Coexpression of Id1 with Bcl2 resulted in acini that were large and had filled lumen, as well as being more disorganized and asymmetrical than acini coexpressing oncogenes HPV-E7 and Bcl2. This provides evidence for additive transformation induced by Id1 and Bcl2 and also suggests some synergy leading to loss of organization. Previously, cooperation between the Id1 paralogue, Id3, and Bcl2 has been observed, where the overexpression of the two genes together alleviated an Id3-induced decrease in colony-forming efficiency and led to cell immortalization (42).

In summary, we have identified that Id1 is indeed expressed in mammary epithelium and is the target of complex regulation during mammary epithelial differentiation. Our data further indicate that overexpression of Id1 can alter acinar development in a manner dependent on cyclin D1 and via an as yet unidentified binding partner. It is thus increasingly clear that Id1 has a potential role in early breast cancer proliferation, in addition to its strong

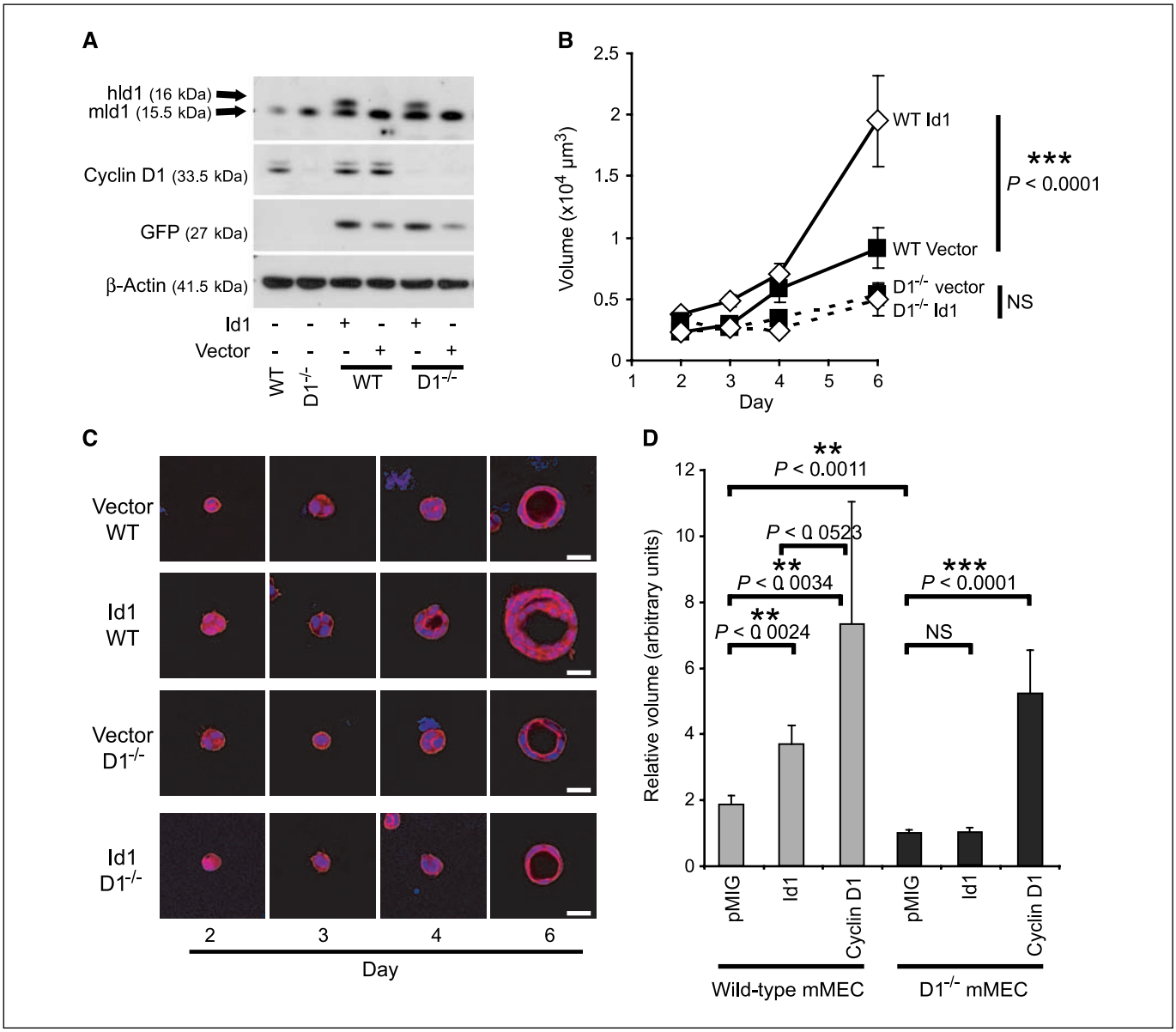

Figure 6. Overexpression of Id1 is not able to promote proliferation on a cyclin D1$^{-/-}$ background. Primary mouse mammary epithelial cells isolated from either wild-type or cyclin D1$^{-/-}$ mice were infected with either Id1 or vector control retrovirus and three-dimensionally cultured on Matrigel for a time course of 6 d. Representative of two experiments. *A,* protein lysates from each cell line were immunoblotted with α-Id1, α-cyclin D1, and α-GFP. β-Actin immunoblotting was used to indicate equal loading. *B,* the volume of wild-type or cyclin D1$^{-/-}$ primary mouse epithelial acini overexpressing Id1 was determined using Leica software on a confocal microscope. For each time point, the diameters through the largest confocal cross section of at least 100 structures were measured and the volume was calculated. *Bars,* SE. *C,* acini were fixed and stained with phalloidin (*red*) and ToPro3 (*blue*) and subsequently imaged with a confocal microscope. Representative cross-section images of acini at each time point. *Bar,* 20 μm. *D,* cyclin D1 overexpression increases the size of cyclin D1$^{-/-}$ and wild-type acini. Cyclin D1$^{-/-}$ and wild-type mouse mammary epithelial cells (*mMEC*) were infected with retrovirus to overexpress cyclin D1, Id1, and vector, and acinar size was determined using Leica software on a confocal microscope. For each time point, the diameters through the largest confocal cross section of at least 60 structures were measured and the volume was calculated. *Bars,* SE.

association with invasion and angiogenesis. Whereas there is very little information on the expression of Id1 in early breast cancer, the detection of some Id1 expression in ductal carcinoma *in situ* and low-grade breast cancers is consistent with an early selection for Id1 expression, at least in some breast cancers (11, 12, 15, 18). Moreover, Id1 was identified as part of a subset of a lung metastasis gene signature that was also present during primary tumor development (17). In that model, the knockdown of Id1 resulted in a decrease in primary tumor mass as well as metastatic spread, unlike several genes in the signature that were specific only to lung metastasis (17).

An interesting dichotomy is that the features of Id1 used to promote early transformation in normal mammary epithelial cells seem to be distinct from the features of Id1 that promote metastasis. Id1 accelerated acinar development of normal mammary epithelial cells, but we did not observe any effect on invasion or disaggregation of cells. By contrast, in studies on metastatic breast cancer cell lines, the down-regulation of Id1 has only marginal effects on proliferation, but greatly reduces their invasive ability and metastatic spread *in vivo* (11). A likely explanation is that Id1 is an oncogene that promotes distinct outcomes depending on the genetic and cellular context. The integrative model of metastatic development (52) suggests that there are three classes of genes that contribute to metastasis, including "metastatic progression genes" that contribute to both primary tumor formation and metastases (52). Our data imply that Id1 belongs to this class of genes, as we identify a likely proliferative role in early tumor development, in addition to its established role in promoting invasion and angiogenesis during the metastatic process.

Acknowledgments

Received 8/10/2007; revised 1/25/2008; accepted 2/21/2008.

Grant support: Cancer Institute NSW, the National Health and Medical Research Council of Australia, the Australian Cancer Research Foundation (ACRF Unit for the Molecular Genetics of Cancer), and the RT Hall Trust. C.E. Caldon is a Cancer Institute NSW scholar and a recipient of an Australian Postgraduate Award. E.A. Musgrove is a Cancer Institute NSW fellow.

The costs of publication of this article were defrayed in part by the payment of page charges. This article must therefore be hereby marked *advertisement* in accordance with 18 U.S.C. Section 1734 solely to indicate this fact.

We thank the following colleagues: Katrina Blazek for assistance and advice with mMEC culture, Dr. Samantha Oakes and A/Prof. Chris Ormandy for providing fresh frozen mammary gland sections, Mark Pinese for mouse genotyping and assistance with animal experiments, Dr. Tilman Brummer for helpful discussions, and the staff of the Garvan Institute BTF for expert animal care.

References

1. Zebedee Z, Hara E. Id proteins in cell cycle control and cellular senescence. Oncogene 2001;20:8317–25.
2. Swarbrick A, Akerfeldt MC, Lee CSL, et al. Regulation of cyclin expression and cell cycle progression in breast epithelial cells by the helix-loop-helix protein Id1. Oncogene 2005;24:381–9.
3. Desprez P-Y, Hara E, Bissell MJ, Campisi J. Suppression of mammary epithelial cell differentiation by the helix-loop-helix protein Id-1. Mol Cell Biol 1995;15:3398–404.
4. Jankiewicz M, Groner B, Desrivieres S. Mammalian target of rapamycin regulates the growth of mammary epithelial cells through the inhibitor of deoxyribonucleic acid binding Id1 and their functional differentiation through Id2. Mol Endocrinol 2006;20:2369–81.
5. Cheung HW, Ling M-T, Tsao SW, Wong YC, Wang X. Id-1-induced Raf/MEK pathway activation is essential for its protective role against Taxol-induced apoptosis in nasopharyngeal carcinoma cells. Carcinogenesis 2004; 25:881–7.
6. Sikder HA, Devlin MK, Dunlap S, Ryu B, Alani RM. Id proteins in cell growth and tumorigenesis. Cancer Cell 2003;3:525–30.
7. Iavarone A, Lasorella A. ID proteins as targets in cancer and tools in neurobiology. Trends Mol Med 2006; 12:588–94.
8. Ohtani N, Zebedee Z, Huot TJG, et al. Opposing effects of Ets and Id proteins on p16INK4a expression during cellular senescence. Nature 2001;409:1067–70.
9. Prabhu S, Ignatova A, Park ST, Sun XH. Regulation of the expression of cyclin-dependent kinase inhibitor p21 by E2A and Id proteins. Mol Cell Biol 1997;17:5888–96.
10. Ozeki M, Hamajima Y, Feng L, Ondrey FG, Schlentz E, Lin J. Id1 induces the proliferation of cochlear sensory epithelial cells via the nuclear factor-κB/cyclin D1 pathway *in vitro*. J Neurosci Res 2007;85:515–24.
11. Fong S, Itahana Y, Sumida T, et al. Id-1 as a molecular target in therapy for breast cancer cell invasion and metastasis. Proc Natl Acad Sci U S A 2003;100:13543–8.
12. Jang K-S, Han HX, Paik SS, Brown PH, Kong G. Id-1 overexpression in invasive ductal carcinoma cells is significantly associated with intratumoral microvessel density in ER-negative/node-positive breast cancer. Cancer Lett 2006;244:203–10.
13. Schoppmann SF, Schindl M, Bayer G, et al. Overexpression of Id-1 is associated with poor clinical outcome in node negative breast cancer. Int J Cancer 2003;104:677–82.
14. Perk J, Gil-Bazo I, Chin Y, et al. Reassessment of Id1 protein expression in human mammary, prostate, and bladder cancers using a monospecific rabbit monoclonal anti-Id1 antibody. Cancer Res 2006;66:10870–7.
15. Lin CQ, Singh J, Murata K, et al. A role for Id-1 in the aggressive phenotype and steroid hormone response of human breast cancer cells. Cancer Res 2000; 60:1332–40.
16. Desprez P-Y, Lin CQ, Thomasset N, Sympson CJ, Bissell MJ, Campisi J. A novel pathway for mammary epithelial cell invasion induced by the helix-loop-helix protein Id-1. Mol Cell Biol 1998;18:4577–88.
17. Minn AJ, Gupta GP, Siegel PM, et al. Genes that mediate breast cancer metastasis to lung. Nature 2005; 436:518–24.
18. Gupta GP, Perk J, Acharyya S, et al. ID genes mediate tumor reinitiation during breast cancer lung metastasis. Proc Natl Acad Sci U S A 2007;104:19506–11.
19. de Candia P, Solit DB, Giri D, et al. Angiogenesis impairment in Id-deficient mice cooperates with an Hsp90 inhibitor to completely suppress HER2/neu-dependent breast tumors. Proc Natl Acad Sci U S A 2003;100:12337–42.
20. Tsuchiya T, Okaji Y, Tsuno NH, et al. Targeting Id1 and Id3 inhibits peritoneal metastasis of gastric cancer. Cancer Sci 2005;96:784–90.
21. Fong S, Debs RJ, Desprez P-Y. Id genes and proteins as promising targets in cancer therapy. Trends Mol Med 2004;10:387–92.
22. Ramaswamy S, Ross KN, Lander ES, Golub TR. A molecular signature of metastasis in primary solid tumors. Nat Genet 2003;33:49–54.
23. van't Veer LJ, Dai H, van de Vijver MJ, et al. Gene expression profiling predicts clinical outcome of breast cancer. Nature 2002;415:530–6.
24. Weigelt B, Hu Z, He X, et al. Molecular portraits and 70-gene prognosis signature are preserved throughout the metastatic process of breast cancer. Cancer Res 2005;65:9155–8.
25. Bernards R, Weinberg RA. Metastasis genes: a progression puzzle. Nature 2002;418:823.
26. Weigelt B, Peterse JL, van't Veer LJ. Breast cancer metastasis: markers and models. Nat Rev Cancer 2005;5: 591–602.
27. Debnath J, Brugge JS. Modelling glandular epithelial cancers in three-dimensional cultures. Nat Rev Cancer 2005;5:675–88.
28. Van Parijs L, Refaeli Y, Lord JD, Nelson BH, Abbas AK, Baltimore D. Uncoupling IL-2 signals that regulate T cell proliferation, survival, and Fas-mediated activation-induced cell death. Immunity 1999;11:281–8.
29. Trausch-Azar JS, Lingbeck J, Ciechanover A, Schwartz AL. Ubiquitin-proteasome-mediated degradation of Id1 is modulated by MyoD. J Biol Chem 2004;279: 32614–9.
30. Makita J, Kurooka H, Mori K, Akagi Y, Yokota Y. Identification of the nuclear export signal in the helix-loop-helix inhibitor Id1. FEBS Lett 2006;580:1812–6.
31. Debnath J, Muthuswamy SK, Brugge JS. Morphogenesis and oncogenesis of MCF-10A mammary epithelial acini grown in three-dimensional basement membrane cultures. Methods 2003;30:256–68.
32. Brummer T, Schramek D, Hayes VM, et al. Increased proliferation and altered growth factor dependence of human mammary epithelial cells overexpressing the Gab2 docking protein. J Biol Chem 2006;281:626–37.
33. Fantl V, Stamp G, Andrews A, Rosewell I, Dickson C. Mice lacking cyclin D1 are small and show defects in eye and mammary gland development. Genes Dev 1995;9: 2364–72.
34. Davison EA, Lee CSL, Naylor MJ, et al. The cyclin-dependent kinase inhibitor p27Kip1 regulates both DNA synthesis and apoptosis in mammary epithelium but is not required for its functional development during pregnancy. Mol Endocrinol 2003;17:2436–47.
35. Parrinello S, Lin CQ, Murata K, et al. Id-1, ITF-2, and Id-2 comprise a network of helix-loop-helix proteins that regulate mammary epithelial cell proliferation, differentiation, and apoptosis. J Biol Chem 2001; 276:39213–9.
36. Uehara N, Chou Y-C, Galvez J, et al. Id-1 is not expressed in the luminal epithelial cells of mammary glands. Breast Cancer Res 2003;5:R25–9.
37. Desprez P-Y, Sumida T, Coppe JP. Helix-loop-helix proteins in mammary gland development and breast cancer. J Mammary Gland Biol Neoplasia 2003;8:225–39.
38. Lingbeck JM, Trausch-Azar JS, Ciechanover A, Schwartz AL. E12 and E47 modulate cellular localization and proteasome-mediated degradation of MyoD and Id1. Oncogene 2005;24:6376–84.
39. Hasskarl J, Duensing S, Manuel E, Munger K. The helix-loop-helix protein ID1 localizes to centrosomes and rapidly induces abnormal centrosome numbers. Oncogene 2004;23:1930–8.
40. Coppe J-P, Smith AP, Desprez P-Y. Id proteins in epithelial cells. Exp Cell Res 2003;285:131–45.
41. Reginato MJ, Mills KR, Becker EBE, et al. Bim regulation of lumen formation in cultured mammary

epithelial acini is targeted by oncogenes. Mol Cell Biol 2005;25:4591–601.
42. Norton JD, Atherton GT. Coupling of cell growth control and apoptosis functions of Id proteins. Mol Cell Biol 1998;18:2371–81.
43. Debnath J, Mills KR, Collins NL, Reginato MJ, Muthuswamy SK, Brugge JS. The role of apoptosis in creating and maintaining luminal space within normal and oncogene-expressing mammary acini. Cell 2002;111: 29–40.
44. Belletti B, Drakas R, Morrione A, et al. Regulation of Id1 protein expression in mouse embryo fibroblasts by the type 1 insulin-like growth factor receptor. Exp Cell Res 2002;277:107–18.
45. Kalas W, Yu JL, Milsom C, et al. Oncogenes and angiogenesis: down-regulation of thrombospondin-1 in normal fibroblasts exposed to factors from cancer cells harboring mutant Ras. Cancer Res 2005;65: 8878–86.
46. Yu Q, Ciemerych MA, Sicinski P. Ras and Myc can drive oncogenic cell proliferation through individual D-cyclins. Oncogene 2005;24:7114–9.
47. Yu Q, Geng Y, Sicinski P. Specific protection against breast cancers by cyclin D1 ablation. Nature 2001;411: 1017–21.
48. Lasorella A, Iavarone A. The protein ENH is a cytoplasmic sequestration factor for Id2 in normal and tumor cells from the nervous system. Proc Natl Acad Sci U S A 2006;103:4976–81.
49. Kolligs FT, Nieman MT, Winer I, et al. ITF-2, a downstream target of the Wnt/TCF pathway, is activated in human cancers with b-catenin defects and promotes neoplastic transformation. Cancer Cell 2002;1: 145–55.
50. Di K, Ling M-T, Tsao SW, Wong YC, Wang X. Id-1 modulates senescence and TGF-b1 sensitivity in prostate epithelial cells. Biol Cell 2006;98: 523–33.
51. Ling M-T, Wang X, Lee DT, Tam PC, Tsao S-W, Wong Y-C. Id-1 expression induces androgen-independent prostate cancer cell growth through activation of epidermal growth factor receptor (EGF-R). Carcinogenesis 2004;25:517–25.
52. Nguyen DX, Massague J. Genetic determinants of cancer metastasis. Nat Rev Genet 2007;8:341–52.